Articles

Functional Analysis of Amino Acid Residues Essential for Activity in the Na^+/H^+ Exchanger of Fission Yeast†

Pavel Dibrov,‡ Paul G. Young,§ and Larry Fliegel*,‡

Department of Biochemistry, 347 Medical Science Building, University of Alberta, Edmonton, Alberta, Canada T6G 2H7, and Department of Biology, Queen's University, Kingston, Ontario, Canada K7L 3N6

Received January 20, 1998; Revised Manuscript Received April 1, 1998

ABSTRACT: We identified amino acid residues important for activity of sod2, the Na^+/H^+ antiporter of *Schizosaccharomyces pombe*. We mutated all eight His residues of sod2 into Arg. Only His367→Arg affected function and resulted in complete inability of sod2 to allow growth of *S. pombe* in LiCl-containing medium. Mutant *S. pombe* (H367R) could not expel sodium in acidic (pH 4.0) medium and were defective in their ability to alkalinize external medium. When His367 was replaced by Asp, sodium export of *S. pombe* was suppressed at acidic pH while the sodium-dependent proton influx at pH 6.1 was increased compared to wild type. We also mutated three residues conserved in putative membrane regions of various eukaryotic and prokaryotic Na^+/H^+ exchangers. *S. pombe* containing Asp241→Asn and Asp266,267→Asn mutations had greatly impaired growth in LiCl-containing medium. In addition, sodium-dependent proton influx at external pH 6.1 was impaired. Sodium export from *S. pombe* cells at external pH 4.0 was also almost completely abolished by the D266,267N mutation; however, the D241N mutant protein retained almost normal Na^+ export. The results demonstrate that His367, Asp241, and Asp266,267 are important in the function of the eukaryotic Na^+/H^+ exchanger sod2.

Na^+/H^+ antiporters are integral membrane proteins residing in the plasma membranes of different cells. They fall into two distinct classes depending on their physiological role. One type of Na^+/H^+ exchanger in vertebrates normally functions to remove excess internal acid from the cytoplasm in exchange for external sodium ions. The sodium gradient created by Na^+/K^+ ATPase serves as the energy source to drive this process (*1*, *2*). Another class of Na^+/H^+ antiporters functions in a similar fashion but normally transports ions in the opposite direction. Bacterial Na^+/H^+ antiporters normally expel intracellular Na^+ by using the preexisting protonmotive force (*3*).

The main bacterial Na^+/H^+ antiporter of *Escherichia coli* is NhaA (*3*). His225 of NhaA determines the pH profile of activity of the protein whereas the other seven His residues are not essential for NhaA function (*4*, *5*). Substitution of His225 with an acidic residue (Asp) shifts the pH optimum of NhaA activity toward a more alkaline pH. Substitution of His225 with a basic residue (Arg) results in a more acidic pH optimum of activity of the protein. The H225A mutation inactivates the antiporter almost completely (*6*). While one His residue is important in the pH activity profile of NhaA, mutation of His residues in the mammalian Na^+/H^+ antiporter does not affect H^+ transport (*7*). Thus, there appears to be a clear difference in the mechanism by which some types of Na^+/H^+ antiporter regulate their pH optimum and in the functional role of His residues in these proteins.

The mechanism of cation coordination by Na^+/H^+ antiporters is an important basic scientific problem which still has to be resolved. Intuitively, one might search for homologous regions between the various types of antiporters for conserved residues which are critical to this function. However, although there is a high degree of sequence conservation within some related species, between more distant species types there is no strong homology. Even between some different kinds of Na^+/H^+ antiporters in the same species there is no apparent homology (*3*).

Another way to determine how Na^+/H^+ antiporters bind cations is to examine a few critically conserved residues which may be adequate to carry out this function. Negatively charged residues located in transmembrane segments are good candidates for binding and translocation of cations and could coordinate Na^+ and H^+ binding (*8*). Three Asp residues have been shown to be crucial for Na^+/H^+ antiport by NhaA in *E. coli* (*9*) and by a related protein in *Vibrio alginolyticus* (*10*). These negatively charged residues are conserved in position in these two species and are located in neighboring transmembrane segments of the protein. It is noteworthy that His225, which functions as a pH sensor in NhaA, is the first His residue following the paired Asp residues.

† This work was supported by a Collaborative Research Grant from the Natural Sciences and Engineering Research Council of Canada and by MRC Program Grant PG-11440.

* Corresponding author.
‡ University of Alberta.
§ Queen's University.

S0006-2960(98)00145-7 CCC: $15.00
Published on Web 05/19/1998

We previously identified sod2 as the Na^+/H^+ antiporter present in the fission yeast *Schizosaccharomyces pombe*. Sod2 was the sole molecular mechanism that removed Na^+ ions from the cytoplasm at the expense of the proton gradient (*11*). Related homologous proteins have now been documented in *Zygosaccharomyces rouxii* (*12*) and in *Saccharomyces cerevisiae* (*13*). Although there is no significant overall homology between sod2 and NhaA (*11*), we note that sod2 contains an acidic transmembrane residue (D241) followed by a pair of acidic transmembrane residues (D266, D267). In addition, there is a His residue that is located 100 amino acid residues downstream of the paired acidic residues (H367). It is therefore possible that some functional analogy occurs between bacterial prokaryotic and fungal eukaryotic Na^+/H^+ antiporters. The residues critical for transport and for the pH optimum of the proteins may be distributed in similar locations within the membrane executing analogous functions.

To test this hypothesis, we performed mutational analysis of sod2. All His residues of sod2 as well as the three Asp residues described above were modified by site-specific mutagenesis. The data show that these four residues are critical in the activity of the Na^+/H^+ exchanger of fission yeast and suggest that there is a functional analogy with similarly placed residues of NhaA. This study represents the first analysis, in eukaryotes, of conserved amino acid residues found important in the activity of prokaryotic Na^+/H^+ antiporters. Our data support the idea that these residues are important in cation transport in a yeast Na^+/H^+ exchanger.

MATERIALS AND METHODS

Yeast Strains and Media. *S. pombe* bearing the *sod2* gene disruption (*sod2*::*ura4*) was used as a host for all transformations and as a control strain (*11*). It was maintained on yeast extract adenine (YEA) or low sodium KMA medium using standard procedures. KMA medium contained (per liter): potassium hydrophthalate, 3 g; K_2HPO_4, 3 g; yeast nitrogen base without amino acids, 7 g; glucose, 20 g; adenine, 100 mg; and histidine, 100 mg. Leucine (200 mg/mL) was added to maintain the *sod2*::*ura4* strain that was not transformed with leu2-containing plasmids.

Site-Directed Mutagenesis. Intermediate plasmids used for construction are described below. Site-directed mutagenesis of residues H12, H54, H67, H98, H233, H376, H424, H429, D241, D266, and D267 of sod2 was performed using the Transformer Site-Directed Mutagenesis Kit (ClonTech, version 2) as recommended by the manufacturer. All mutations were designed to create or remove a restriction enzyme site that could be easily detected in the subsequent analysis. The following oligonucleotides were used to produce the desired gene alterations; the names correspond to the mutations-mutated bases are shown in boldface type, and the alteration in the restriction enzyme site follows. The oligonucleotides are as follows: H12R, 5′-A GAC AAA GTC C**gc** TTA GCT TTA ATA GTG-3′, new *Dde*I site; H54R, 5′-A TTT GGG CCT C**gc** GCT GCT AAA CTC GTA GA-3′, new *Hha*I site; H67R, 5′-C CCT TTT TCC TGG GGT GAC C**g**T GGA GAT TAC TTG-3′, removed a *Nco*I site; H98R, 5′-GCA TAT TTT CA**g** C**gc** AAT TTT CGA AGC ATC ATT G-3′, new *Hha*I site; H233Rr, 5′-TTT CTG AGC G**c**G CTT TAA AAT GAA CG-3′, new *Hha*I site; H367Rr, 5′-TAT TGG TCC GAA A**c**G **g**CC AAC GAA AAG GGC-3′, new *Hae*III site; H424/429Rr, 5′-CA AAT CAC TAA TAC A**c**G GAT ACT GAA ACC **gc**G **c**AC AAT GAT TG-3′ (double mutation), new *Hha*I site; H367Dr, 5′-CCC TAT TGG **g**CC GAA AT**c** TCC AAC GAA AAG GGC-3′, new *Hae*III site; H367Ar, 5′-CC TAT TGG TCC GAA A**gc** TCC AAC GAA AAG GGC-3′, *Alu*I site; D241Nr, 5′-G CGG AAG GGA ATA ATA **g**CT AAT AGC AT**t** AAT TAA ACG GTA T-3′, new *Alu*I site; and D266,-267N, 5′-GGA ACT ATT ATT GGA GTT **a**A**c** **a**AC CTG TTG ATG TCC TTT TTT GC-3′ (a double mutation), with a new *Hinc*II site. Oligonucleotides with the "r" designation indicate that the oligonucleotide encodes for the complementary DNA strand.

The template for mutagenesis was the plasmid p*KS*-*sod2* that contains the *sod2* gene as a 2.3 kb *Hind*III fragment together with the 187 bp upstream and 692 bp downstream flanking regions (*11*). Mutated double-stranded DNA was transformed into the *mut*S strain of *E. coli* (BMH 71-18). The standard trans oligo *Sca*I/*Stu*I (ClonTech) was used as a selection primer in all mutagenesis reactions. After selective digestion of the mixed plasmid pool with *Sca*I, the plasmid was propagated in *E. coli* DH5α. The transformant clones were screened by digestion with enzymes whose sites were created/eliminated by the mutagenic primers. Plasmid DNA from the selected clones was isolated and digested with the following enzymes to excise the minimal *sod2* gene fragments containing the desired mutation. *Bsg*I and *BspE*I were used to obtain a 430 bp fragment with the H367 mutation and the H424,429R mutation. *Nco*I and *Nhe*I were used to obtain a 549 bp fragment containing the D241N, H67R, H98R, and H233R mutations. The combination of *Nhe*I with *BspE*I excised a 312 bp insert containing the double D266,267N mutation. The enzymes *Sal*I and *Nco*I were used to obtain a 476 bp insert with the H12R or H54R mutation. Mutated fragments were then used to replace the respective sequences in pSK-*sod2*. After verification by DNA sequencing, the HA tag was introduced at the 3′-terminus of the *sod2* gene as described below. HA-tagged variants were made for the wild-type *sod2*, as well as for the mutants H367A, H367D, H367R, D241N, and D266,-267N.

Addition of the Hemagglutinin (*HA*) *Tag to the 3′-Terminus of the sod2 Gene*. The addition of the HA tag at the 3′-terminus of sod2 was as described earlier (*14*). Briefly, the plasmid pARTA was made by an exchange of *Swa*I−*Swa*I fragments that added the HA tag to the wild-type *sod2* cloned in pSOD2.11 (*11*) where it is controlled by the strong ADH promoter. The purpose of this construct was to have a positive control for immunoblotting experiments since we found that expression from the endogenous *sod2* promoter was only at low levels. In this work, the 813 bp *Swa*I−*Swa*I fragment containing the HA tag was ligated into a series of pSK-*sod2* vectors carrying the wild-type or mutated form of *sod2*. Finally, tagged variants of the *sod2* gene were cloned into the pWH5 shuttle vector (*15*) as *Hind*III−*Hind*III inserts for expression in the *S. pombe sod2*::*ura4* strain.

Growth Rate Assessment. The lithium tolerance of various transformants was determined at different pHs in liquid KMA medium that was supplemented with the indicated amounts of LiCl. Because the pH of the medium tended to change

with cell growth, it was buffered with a variety of buffers that were at a final concentration of 0.1 M. The buffers were citrate/Mes (pH 3.0, 3.5, 4.5, and 5.0); succinate/Mes (pH 4.0, 5.5, and 6.0); and Mes/Trizma base (pH 6.5 and 7.0). Leucine (200 mg/mL) was added for growth of the *sod2*::*ura4* strain. To assess growth, 2×10^6 cells were inoculated into 2 mL of medium and incubated at 30 °C with vigorous aeration for 24 h or where specified for 48 h. Growth was then assessed by measuring the increase in absorbance of the cell suspension at 600 nm. The pH of the culture medium was assessed after cell growth, and in all cases, the growth medium was not acidified more than 0.10−0.15 pH unit. The results presented are typical of at least three experiments for each *S. pombe* strain, and the standard deviation was approximately 15%.

^{22}Na Transport. The activity of sod2 at an external pH of 4.0 was measured as described previously (*11*) with minor modifications. Cells were grown in KMA medium and harvested at a cell density of approximately 5×10^6 cells/mL. They were washed twice with double-distilled water, and resuspended in loading buffer (10 mM NaCl, 20 mM Mes−Tris, pH 7.0) at 10^9 cells/mL. After addition of 0.5 mCi/mL carrier-free ^{22}Na, cells (1 mL) were gently rotated at room temperature for 1 h. ^{22}Na-loaded cells were briefly pelleted, washed with the same volume of loading buffer without isotope, and diluted quickly into 20 mL of ^{22}Na-free loading buffer of pH 4.0. At the indicated times, 1.5 mL aliquots of the cell suspension were withdrawn, filtered immediately through the 0.8 μm pore-size Millipore AA filters, and washed with 5.0 mL of double-distilled water. The radioactivity of filters was measured with a β-counter. Cells treated with 0.2% saponin for 10 min were used to subtract nonspecific absorption of the isotope.

Measurement of Proton Uptake. Na^+-dependent H^+ uptake in different *S. pombe* strains was measured as described in ref *16*, *17* with minor modifications. Approximately 10^7 cells/mL in the logarithmic phase of growth were washed twice with double-distilled water. They were then resuspended at a density of 5×10^8 cells/mL in 20 mM Mes/Tris (pH 6.1) with or without 100 mM NaCl. After 2 h of incubation at room temperature, cells were briefly pelleted in a microfuge and concentrated 5-fold in 0.5 mL of 1 mM Mes/Tris (pH 6.1). They were quickly added to 2 mL of the same buffer in a stirred cuvette, and the pH was measured using a Fisher Scientific Accumet 925 pH meter. Data were collected with an Apple Macintosh SE computer.

Membrane Isolation. Plasma membrane-enriched fractions from *S. pombe* were prepared essentially as described earlier (*18*) with minor modifications (*19*). Yeast cells were grown aerobically in KMA medium to an OD_{600} of 1.5 at 30 °C, and other procedures were carried out at 0−4 °C. After pelleting and washing with double-distilled water, cells were resuspended at a concentration of 5×10^9 cells/mL in disruption buffer [50 mM Tris/HCl, pH 7.5, 0.3 M sucrose, 5 mM EDTA, 1 mM EGTA, 5 mg/mL bovine serum albumin, protease inhibitor cocktail (*20*), and 1 mM dithiothreitol] and passed through a French Press at 20 000 psi. Unbroken cells were pelleted by centrifugation at 3500*g* for 5 min, and the supernatant was centrifuged at 14000*g* for 20 min. Membranes were then pelleted at 200000*g* for 1 h and resuspended in 1 mM EGTA−Tris (pH 7.5), 10% glycerol using a glass homogenizer with a Teflon plunger.

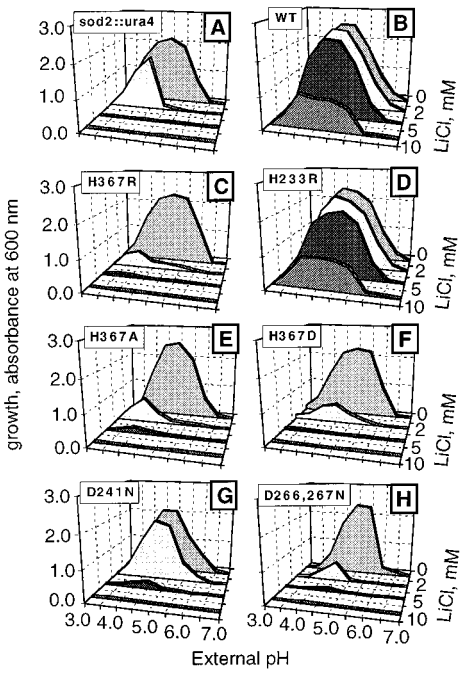

FIGURE 1: LiCl tolerance in wild-type and *sod2* mutants at various external pHs. The ordinate represents growth (OD_{600}nm) in liquid minimal medium for 24 h (A−F) or 48 h (G−H), measured as described under Materials and Methods. LiCl tolerance was measured in disrupted *sod2*::*ura4* mutant (A), in the same mutant transformed with pWH5 bearing wild-type *sod2* (B), and in a series of *sod2* mutants introduced into *sod2*::*ura4* with pWH5-*sod2* derivatives carrying the respective mutations (C−H): H367R (C); H233R (D); H367A (E); H367D (F); D241N (G); D266,267N (H).

The membrane suspension was centrifuged as before, and finally resuspended in a small volume of 1 mM EGTA−Tris (pH 7.5), 10% glycerol.

Electrophoretic Methods. Yeast membranes were pre-extracted and solubilized using dodecyl maltoside as described earlier (*21*). Proteins were resolved using a 12% polyacrylamide gel and were visualized using Coomassie Blue staining. Western blotting and immunoblotting were performed essentially as described earlier (*14*). Anti-HA monoclonal antibody 12CA5 (Boehringer Mannheim, Laval, Quebec, Canada) was used at a dilution of 1:500, and peroxidase-conjugated goat anti-mouse antibody (Bio/Can, Mississaugua, ON) was used at a dilution of 1:2000. Immunoreactive proteins were visualized using the Amersham Enhanced Chemiluminescence kit as described by the manufacturer.

RESULTS

Lithium Resistance in Different sod2 Mutants as a Function of External pH. The sod2 protein functions to remove internal sodium; however, it can also transport lithium ions in exchange for protons (*11*). This makes it possible to assess functional effects of different mutations of sod2 in vivo by measuring lithium tolerance in intact *S. pombe*. Since Li^+ is much more toxic to cells than Na^+, one can use relatively low LiCl concentrations that eliminate possible osmotic effects. Figure 1 (panel A) confirms that the *sod2*::*ura4* disruption mutant is highly sensitive to external lithium. LiCl at a concentration exceeding 2 mM completely arrests growth in the pH range of 3.5−6.5. Transformation of the *sod2*::*ura4* strain with the plasmid carrying wild-type *sod2* restores

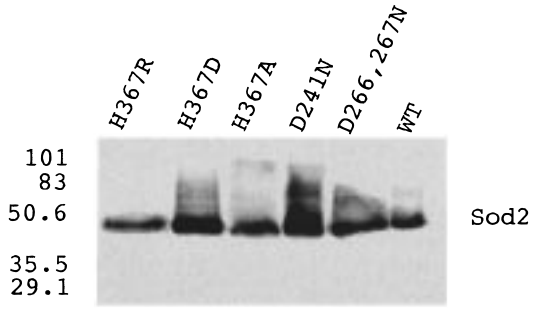

FIGURE 2: Immunodetection of sod2 protein in *S. pombe* plasma membranes. Membranes were solubilized with dodecyl maltoside and analyzed using SDS−PAGE followed by immunoblotting with anti-HA antibodies as described in (*14*). Three hundred micrograms of total membrane protein was loaded per lane.

resistance to as much as 10 mM LiCl within the same pH range (Figure 1B). The H367R mutation of sod2 affects the restoration of LiCl resistance markedly. It is as sensitive to LiCl as the *sod2*::*ura4* disruption mutant (Figure 1C). Replacements of the other seven His residues of sod2 with Arg did not change lithium tolerance in transformant cells. An example of such a 'neutral' His substitution (H233R mutant) is shown in Figure 1D. There was no difference in sensitivity to LiCl between this mutant and cells transformed with the wild-type *sod2* plasmid. To characterize the role of His367 further, it was mutated to an Ala and an Asp residue. Replacement with either Ala (Figure 1E) or an Asp (Figure 1F) followed by transformation into *sod2*::*ura4* cells resulted in yeast that were sensitive to external Li^+ at all pHs.

In the next series of experiments, three Asp residues located in putative transmembrane segments of the sod2 protein were substituted with the uncharged analogue Asn. In the bacterial antiporter, the same change in aspartate residues within this conserved motif inactivates the protein (*9*, *10*). When sod2 was mutated and transformed into the *sod2*::*ura4* strain, lithium tolerance was not restored in cells carrying either the D241N (Figure 1G) or the D266,267N (Figure 1H) mutation in sod2.

Expression of sod2 Mutants. We examined expression of the various sod2 mutants to confirm that they were expressed and correctly targeted. We added the highly immunoreactive hemagglutinin (HA) tag to the carboxyl terminal of the protein as described earlier (*14*) and then examined expression under control of the endogenous sod2 promoter. The tag was added to the control and to sod2 mutants that exhibited significant changes in phenotype (wild type; H367R, H367A, H367D; D241N and D266,267N). We used monoclonal anti-HA antibody to examine the level of the sod2 mutant proteins in membrane preparations from transformants of *sod2*::*ura4* (Figure 2). In all cases analyzed, the mutations introduced did not prevent either synthesis of sod2 or its membrane targeting. Therefore, differences in lithium tolerance among the mutant strains could not be attributed to an inability to express the sod2 mutant proteins.

Active ^{22}Na Efflux from the Whole Cells. To examine sod2 function directly in various mutants, we measured ^{22}Na transport in the yeast strains. Cells were preloaded with ^{22}Na at pH 7.0, briefly washed, and quickly transferred into isotope-free medium of pH 4.0. Sodium efflux was assessed in the *sod2*::*ura4* strain transformed with either wild-type

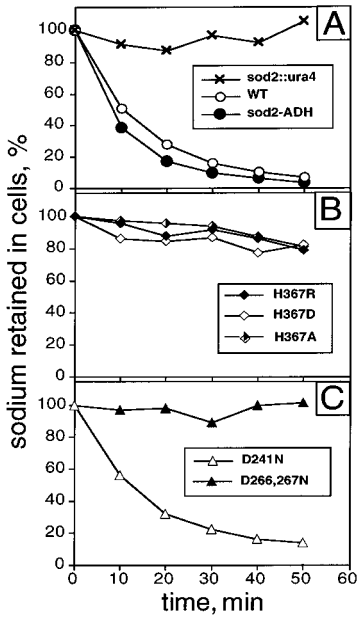

FIGURE 3: Active sodium transport in intact *S. pombe*. Cells were equilibrated with $^{22}Na^+$ (0.5 μCi/mL) for 1 h in the presence of 10 mM unlabeled NaCl at pH 7.0. $^{22}Na^+$ transport at pH 4.0 was monitored by filtration after dilution into $^{22}Na^+$-free medium as described under Materials and Methods. Radioactive Na^+ remaining in the cells is expressed relative to that recorded at $T = 0$ min.

or mutant sod2 genes. Initial results (Figure 3A) confirmed that Na^+ efflux was absent in the disrupted strain while sod2-overexpressing cells demonstrated greater sodium efflux than that of the wild-type cells (Figure 3A). These data confirm that ^{22}Na efflux reflects sod2 function. When we examined the *sod2*::*ura4* strain containing the H367R, H367A, and H367D mutants, we found only residual ^{22}Na export (Figure 3B). Similarly, the D226,227N mutant failed to export ^{22}Na (Figure 3C). In contrast, the D241N-containing strain demonstrated rapid efflux of ^{22}Na. This result was surprising considering that growth of *sod2*::*ura4* containing this mutant was inhibited by the addition of lithium (Figure 1G).

Na^+-Dependent H^+ Uptake. Sod2 catalyzes coupled transmembrane movements of sodium ions and protons. Therefore, it is possible to measure sod2 activity by measuring proton influx that is driven by an outwardly directed sodium gradient. We used this approach to measure the activity of sod2 at an external pH of 6.1. At this external pH, it is relatively easy to load these cells with considerable amounts of Na^+. We created an artificial ΔpNa^+ (high Na^+ concentration inside the cell) by incubation of cells in medium with 0.1 M NaCl at pH 6.1 and subsequently transferring the cells into the same buffer devoid of NaCl. By monitoring the pH of a weakly buffered external medium, we found that within a few minutes, cells containing the wild-type sod2 exhibit Na^+-dependent proton uptake (Figure 4A, filled symbols). Cells that were not loaded with sodium did not alkalinize the external medium (Figure 4A, empty symbols). In cells bearing sod2 with the H367R (Figure 4B) or the H367A (Figure 4C) mutation, we found no alkalinization of the external medium. However, a rapid proton flux was observed in the H367D mutant cells preloaded with NaCl (Figure 4D). The magnitude of the resulting pH shift was comparable to that produced by wild-type cells. In addition, the H367D mutant alkalinized the experimental medium much faster than the wild type. Both Asp→Asn

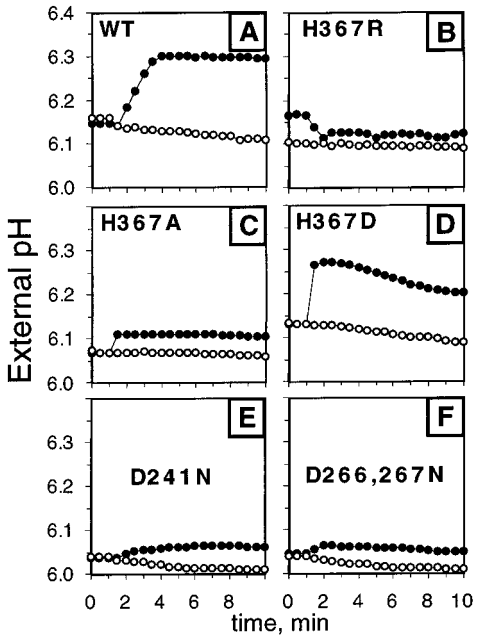

FIGURE 4: Na^+-dependent H^+ fluxes mediated by *S. pombe*. Cells carrying either the wild-type or the mutant sod2 were loaded either with (filled symbols) or without (open symbols) 100 mM NaCl. They were then briefly washed and added to the experimental buffer; H^+ influx was then monitored as described under Materials and Methods. Results are typical of at least three separate experiments. (A) Wild type; (B) H367R; (C) H367A; (D) H367D; (E) D241N; (F) D266,267N.

mutants were not capable of taking up protons in exchange for Na^+ at the external pH of 6.1 (Figure 4E,F).

DISCUSSION

We used site-specific mutagenesis to characterize the activity of several amino acids that we suspected were critical in enzyme activity. We demonstrated that HA-tagged variants of the mutated proteins were expressed normally in the plasma membrane of *S. pombe* (Figure 2). It should be noted that the expression level of sod2 from its own promoter is very low. Thus, it was impossible to visualize the HA-tagged sod2 in total cell lysates without enrichment in membrane preparations. This indicates that very few copies of the antiporter per cell are sufficient to fulfill its physiological function. The same is true for the bacterial Na^+/H^+ antiporter, NhaA (*22*).

To identify amino acids important in the function of sod2, we initially characterized the physiological activity of this Na^+/H^+ antiporter in *S. pombe*. We determined the sensitivity of growth to added LiCl at various pHs in wild type and in a series of sod2 mutants. Too acidic medium is obviously harmful for these cells. However, growth also decreased at more alkaline pHs in our buffered medium (Figure 1). We then examined the growth profiles of *S. pombe* which contained the sod2 mutants. The molecular analysis of sod2 revealed that of all the His residues of sod2, only His367 was critical for function. The H367R, H367A, and H367D mutations all resulted in a dramatic loss in the ability of yeast to grow in LiCl-containing medium (Figure 1). The same mutations also resulted in a complete inability to extrude Na^+ in medium of acidic pH (Figure 3). We noted that only the H367D mutant was able to demonstrate proton uptake in medium of higher pH (Figure 4) even though when Na^+-loaded, it did not extrude Na^+ (Figure 3). A key difference between these experiments was that the measurement of Na^+ extrusion was at an acidic external pH (pH 4.0) while measurement of proton uptake of Na^+-loaded yeast was in medium of pH 6.1. These data suggest that while the H→A replacement inactivates the antiporter, the H→D substitution could be shifting the pH optimum toward a more alkaline pH. Unfortunately, because of the nature of the proton uptake assay and because we were working with whole cells, it was not possible to measure proton uptake at more acid pHs. However, the results are similar to those found earlier with His225 of NhaA (*6*) and suggest that His367 of sod2 could be a functional analogue of His225 of NhaA. A notable difference between the two His residues was that in *E. coli* the H225R mutation shifted the pH optimum of NhaA toward an acidic pH (*6*). However, the H367R-sod2 mutation is inactive in our assays at both acidic (Figure 3B) and more alkaline (Figure 4B) pHs. This discrepancy may be a reflection of the functional differences between the two proteins. NhaA is known to be electrogenic (*23*) while sod2 is electroneutral (*11*). In addition, the bacterial antiporter works at an external pH of 7.0−9.0 while the yeast protein can operate at much more acidic pHs (Figure 1, and unpublished observations). Thus, while H367 of *S. pombe* and H225 of *E. coli* could be functional analogues, they have significant differences. We suggest that His367 may be part of the proton binding site of sod2 and that it is part of a characteristic Na^+/H^+ antiporter denominator. It has a characteristic position being the first His residue located downstream of the double Asp pair and is near the membrane−water interface. This suggestion is based on our results and on those of Rimon et al. with His225 of NhaA (*24*). It was initially suggested that His225 of NhaA functions as an internal pH sensor (*4*, *6*). However, recent evidence supports a periplasmic location for this residue (*5*, *25*), making it more likely to serve in proton binding and transport.

We also examined the function of three Asp residues with analogous positions in bacterial and yeast Na^+/H^+ exchangers. The double mutation D266,267N inactivated sod2 similar to residues D163,164 of NhaA. In contrast, we found that cells containing the D241-sod2 mutant had almost the normal rate of ^{22}Na efflux at acidic pH 4.0 (Figure 3C) but were unable to perform Na^+-coupled proton transport at pH 6.1 (Figure 4E). We note, however, that the residual activity left in this mutant was unable to provide effective protection against Li^+ ions in intact yeast and over a broad range of external pH (Figure 1G). Therefore, D241 appears to be important for optimum sod2 activity in whole cells, but the antiporter still demonstrates activity with the D→N mutation. It is clear that some sodium transport capability still remains, yet proton uptake is below normal. It is possible that this mutant can now facilitate Na^+-Na^+ exchange but not Na^+-H^+ exchange. Alternatively, Na^+ movement by the D241 mutant may be unidirectional and uncoupled from H^+ fluxes. The exact nature of the effect of the D241 mutation has yet to be elucidated.

Figure 5 is a comparison of protein sequences occurring in various prokaryotic and yeast Na^+/H^+ antiporters. The motif of a membrane-associated Asp residue followed by a pair of membrane-associated Asp residues is present in all NhaA-like proteins and in yeast Na^+/H^+ antiporters. This

S. entiritidis	126	WAIPAAT**D**IAFALG	(4)	156	LMALAII**DD**LGA	(5) (27)
V. alginolyticus	118	WAIPAAT**D**IAFALG	(4)	148	LLALAII**DD**LGV	(5) (28)
E. coli (NhaA)	126	WAIPAAT**D**IAFALG	(4)	156	LMALAII**DD**LGA	(5) (9)
Z. rouxii	233	AEGKRII**D**RESFLA	(7)	258	FGSMLGV**DD**LLV	(8) (12)
S. cerevisiae	236	AEKKNII**D**RESFLA	(7)	261	FGSILGV**DD**LLV	(8) (13)
S. pombe (sod2)	234	AQKYRLI**D**AISYYS	(7)	259	IGTIIGV**DD**LLM	(8) (11)

FIGURE 5: Alignment of prokaryotic and eukaryotic Na^+/H^+ antiporters. Boldface residues indicate conserved amino acids that may be important in cation binding. Numbers preceding sequences indicate the number of the first amino acid in the sequence shown. Numbers in parentheses following the sequence indicate the putative transmembrane segment in which the fragment is found or is associated with. The isoforms' topology was assigned according to the indicated reference. Reference numbers are at the end of each line. For *S. pombe*, the topology was assigned using the program Topopredict II (*29*).

occurs despite the absence of extensive homology between other residues of these regions (*9*−*13*, *26*, *27*). It is noteworthy that in all the bacterial NhaA-like proteins, there is a residue equivalent to His367 of sod2, approximately 60 residues downstream of the double Asp pair. We suggest that a "3D-motif"—a single membrane-associated Asp residue followed by a later membrane pair of Asp residues—is an important conserved element involved in Na^+-dependent proton transport. This is based on our observed functional effects of mutation of the trio of Asp residues D241 and D266,267. In addition, in NhaA the analogous pair of Asp residues (D163,164) showed similar effects on proton transport. Though mutation of D133 of NhaA did not affect proton fluxes, Na^+ fluxes were not examined in this study (*9*). We also found that the D241N mutation of sod2 retained some activity. It may be that the DD doublet of the motif is the primary element of the Na^+ binding site in both the bacterial and yeast proteins, with the upstream acidic residue providing a supporting though not critical role. Mammalian antiporters may have different amino acids involved in cation coordination. There are no paired acidic residues in the membrane region of mammalian antiporters, and mutation of His residues did not result in similar functional effects on activity (*7*). We suggest that the conserved structure in bacterial and yeast antiporters may serve to coordinate transported cations, possibly in a crown ether-like cluster as hypothesized earlier by Boyer (*28*). The residues involved provide their carboxylate oxygen atoms to coordinate alkali cations and, possibly, protons in the form of H_3O^+ ions. Modest conformational changes in such a structure could result in release of a coordinated cation at the opposite side of the membrane (*28*). This mechanism of cation coordination may be similar to that proposed for the *E. coli* transport protein melibiose permease. In this case, four Asp residues are thought to form a cation binding pocket involved in cation-coupled cotransport of disaccharides (*8*). The residues involved are not necessarily in the middle of the integral membrane region, but may also be in the aqueous environment near the water−membrane interface. This may also be true with sod2, and residues involved in cation transport need not necessarily be embedded centrally within the membrane.

It is possible that some of the effects we observed in this study were due to perturbation of the structure of sod2 rather than more direct effects on cation binding and transport. However, this possibility seems much less likely since the changes in the amino acids were minimal. In addition, the mutant D241N retained partial activity depending on assay conditions. This makes it unlikely that the effects observed were due to any perturbations of the structure of the protein. In the case of His residues, we mutated every His residue in the protein, and only mutation of H367 had any effect on sod2 function. Therefore, it appears clear that at least in these cases, minor changes in one amino acid did not have a major effect on the structure of the protein.

Our study is the first functional analysis of residues important in transport of a yeast Na^+/H^+ exchanger. It suggests that there may be a critical set of polar amino acid residues involved in cation binding and transport. The data do not exclude the possibility that other residues are also involved in antiport mediated by sod2 and related exchangers. Future experiments will examine other amino acid residues important in sod2 function.

ACKNOWLEDGMENT

We are grateful for the assistance of Dr. S. Hemmingsen (Plant Biotechnical Institute, Saskatchewan) and Carmen Harris, Dr. R. S. Haworth, and Dr. E. Dibrov (Department of Biochemistry, University of Alberta).

REFERENCES

1. Fliegel, L., and Dibrov, P. (1996) In *The Na^+/H^+ Exchanger* Fliegel, L., Ed.) pp 1−20, Springer/R. G. Landes Co., Austin, TX.
2. Orlowski, J., and Shull, G. (1996) In *The Na^+/H^+ Exchanger* (Fliegel, L., Ed.) pp 123−148, R. G. Landes Co., Austin, TX.
3. Schuldiner, S., and Padan, E. (1996) In *The Na^+/H^+ Exchanger* (Fliegel, L., Ed.) R. G. Landes Co., Austin, TX.
4. Gerchman, Y., Olami, Y., Rimon, A., Taglicht, D., Schuldiner, S., and Padan, E. (1993) *Proc. Natl. Acad. Sci. U.S.A.* 90, 1212−1216.
5. Olami, Y., Rimon, A., Gerchman, Y., Rothman, A., and Padan, E. (1997) *J. Biol. Chem. 272*, 1761−1768.
6. Rimon, A., Gershman, Y., Olami, Y., Schuldiner, S., and Padan, E. (1995) *J. Biol. Chem. 270*, 26813−26817.
7. Wang, D., Balkovetz, D. F., and Warnock, D. G. (1995) *Am. J. Physiol. 269*, C392−C402.
8. Poolman, B., Knol, J., van der Does, C., Henderson, P. J. F., Liang, W., Leblanc, G., Pourcher, T., and Mus-Veteau, I. (1996) *Mol. Microbiol. 19*, 911−922.
9. Inoue, H., Noumi, T., Tsuchiya, T., and Kanazawa, H. (1995) *FEBS Lett. 363*, 264−268.
10. Nakamura, T., Komano, Y., and Unemoto, T. (1995) *Biochim. Biophys. Acta 1230*, 170−176.
11. Jia, Z. P., McCullough, N., Martel, R., Hemmingsen, S., and Young, P. G. (1992) *EMBO J. 11*, 1631−1640.
12. Watanabe, Y., Miwa, S., and Tamai, Y. (1995) *Yeast*, 829−838.
13. Prior, C., Potier, S., Souciet, J., and Sychrova, H. (1996) *FEBS Lett. 387*, 89−93.
14. Dibrov, P., Smith, J. J., Young, P., and Fliegel, L. (1997) *FEBS Lett. 405*, 119−124.

15. Wright, A., Maundrell, K., Heyer, W. D., Beach, D., and Nurse, P. (1986) *Plasmid 15*, 156−158.
16. Haworth, R. S., and Fliegel, L. (1993) *Mol. Cell. Biochem. 124*, 131−140.
17. Haworth, R. S., Lemire, B. D., Cragoe, E. J. J., and Fliegel, L. (1991) *Biochim. Biophys. Acta 1098*, 79−89.
18. McCusker, J. H., Perlin, D. S., and Haber, J. E. (1987) *Mol. Cell. Biol. 7*, 4082−4088.
19. Nakamoto, J. M., Rao, R., and Slayman, C. W. (1991) *J. Biol. Chem. 266*, 7940−7949.
20. Michalak, M., Fliegel, L., and Wlasichuk, K. (1990) *J. Biol. Chem. 265*, 5869−5874.
21. Silva, N. L. C. L., Haworth, R. S., Singh, D., and Fliegel, L. (1995) *Biochemistry 34*, 10412−10420.
22. Taglicht, D., Padan, E., and Schuldiner, S. (1991) *J. Biol. Chem. 266*, 11289−11294.
23. Taglicht, D., Padan, E., and Schuldiner, S. (1993) *J. Biol. Chem. 268*, 5382−5387.
24. Hahnenberger, K. M., Jia, Z., Fliegel, L., Hemmingsen, S., and Young, P. G. (1996) In *The Na^+/H^+ Exchanger*, (Fliegel, L., Ed.) pp 255−264, R. G. Landes Co., Austin, TX.
25. Rothman, A., Padan, E., and Schuldiner, S. (1996) *J. Biol. Chem. 271*, 32288−32292.
26. Pinner, E., Carmel, O., Bercovier, H., Sela, S., Padan, E., and Schuldiner, S. (1992) *Arch. Microbiol. 157*, 323−328.
27. Nakamura, T., Komano, Y., Itaya, E., Tsukamoto, K., Tsuchiya, T., and Unemotoe, T. (1994) *Biochim. Biophys. Acta 1190*, 465−468.
28. Boyer, P. (1988) *Trends Biochem. Sci. 13*, 5−7.
29. Claros, M. G., and von Heijne, G. (1994) *Comput. Appl. Biosci. 10*, 685−686.

BI9801457